Journal of Hazardous Materials 472 (2024) 134567

Contents lists available at ScienceDirect

Journal of Hazardous Materials

journal homepage: www.elsevier.com/locate/jhazmat

Per- and polyfluoroalkyl substances (PFAS) in construction and demolition debris (CDD): discerning sources and fate during waste management

Yalan Liu [a,b], Ashley Lin [b], Jake Thompson [b], John A. Bowden [b,c], Timothy G. Townsend [b,*]

[a] Department of Civil, Environmental and Geomatics Engineering, Florida Atlantic University, Boca Raton, FL 33431, USA
[b] Department of Environmental Engineering Sciences, University of Florida, PO Box 116450, Gainesville, FL 32611-6450, USA
[c] Department of Department of Physiological Sciences, University of Florida, 1333 Center Drive, Basic Science Building, Room 324, Gainesville, FL 32610, USA

HIGHLIGHTS

- Various PFAS levels detected in CDD components.
- Majority of total available PFAS was from precursor species.
- Leachable PFAS consisted mainly of PFCAs.
- Data were extrapolated to estimate US CDD waste PFAS mass.
- CDD may pose similar or greater leaching risk compared to MSW.

GRAPHICAL ABSTRACT

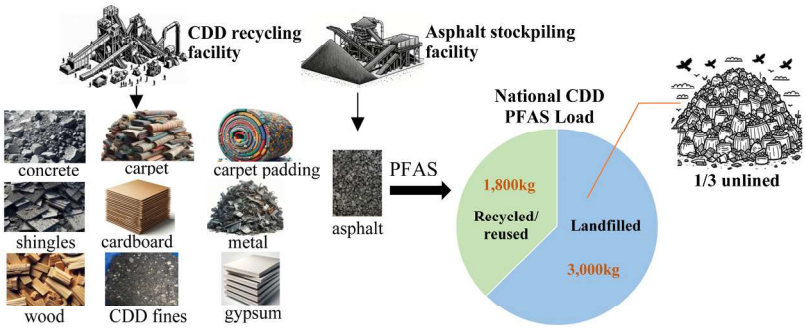

ARTICLE INFO

Keywords:
Landfilling
Waste management
Leaching risk
Drywall
Wood

ABSTRACT

As regulatory frameworks for per- and polyfluoroalkyl substances (PFAS) evolve, the solid waste community seeks to manage PFAS risks effectively. Despite extensive research on PFAS in municipal solid waste (MSW) and wastewater sludge, there is limited information on a major global waste stream which seldom gleans regulatory oversight — construction and demolition debris (CDD). This study sampled a CDD processing facility to provide material-specific information on the PFAS profile within CDD. The bulk CDD accepted by this facility was separated into major categories, representatively sampled, then characterized for total available PFAS ($\sum_{92}$PFAS). As reprocessed CDD is ultimately recycled or landfilled, often unencapsulated or in unlined landfills, the PFAS leaching potential was also examined using two leaching procedures. Among the categories assessed for total PFAS, carpeting, carpet padding, and gypsum drywall showed elevated concentrations compared to other components, with most of the PFAS mass contributed by precursor species. However, materials with the highest total PFAS, such as carpeting, did not necessarily exhibit the highest leaching, and leachate was predominantly composed of terminal species rather than precursors. Extrapolating these findings with national CDD generation and management data inventories suggests that despite MSW having higher total available PFAS concentrations, the leachability of PFAS from landfilled CDD is comparable, raising legitimate concerns with CDD disposal practices, particularly in unlined CDD landfills.

* Corresponding author.
E-mail address: ttown@ufl.edu (T.G. Townsend).

https://doi.org/10.1016/j.jhazmat.2024.134567
Received 18 February 2024; Received in revised form 30 April 2024; Accepted 7 May 2024
Available online 10 May 2024

1. Introduction

Per- and polyfluoroalkyl substances (PFAS) are a group of chemicals of emerging concern because of their environmental persistence, abundance, and toxicity [1,2]. In the last decade, several state and federal agencies have developed risk-based thresholds for PFAS to limit human exposure and environmental release [3-5]. Due to the presence of PFAS in a wide range of industrial and consumer products, a significant portion of PFAS produced ends up in solid waste streams. As regulatory guidance continues to be developed for PFAS, the solid waste community faces the challenge of developing effective waste management strategies to minimize the risk of PFAS exposure and environmental release. While there is a breadth of research focused on PFAS characterization in specific solid waste streams such as municipal solid waste (MSW) [6-9], wastewater sludge [10-12], and paper products [13,14], there is limited information on one of the largest waste streams produced globally — construction and demolition debris (CDD).

Around 544 million metric tons of CDD were generated in the US in 2018; more than twice the amount of MSW [15]. CDD is derived from construction, renovation, and demolition of man-made structures such as buildings, roads, and bridges [16,17]. The composition of CDD varies regionally and between waste generating activities, but it is typically composed of bulky, heavy materials such as concrete, asphalt, wood products, and metals [18]. In countries with established recovery programs, components from construction and demolition projects may be recovered for economic or environmental benefits [19]. Materials with high value markets or reuse feasibility, like concrete and asphalt pavement, are commonly reprocessed onsite or hauled to dedicated stockpiles. Other components (including some fractions of concrete and asphalt) are often sent to a Material Recovery Facility (MRF) dedicated to CDD recovery [19,20]. At these facilities, CDD is separated and reprocessed to generate marketable materials. For example, processed metal, concrete, and asphalt may be recycled into new products or used in a similar manner to the original, whereas untreated wood and CDD fines (a soil-like byproduct of CDD processing) may be repurposed as compost or soil amendment for land application, but inevitably some components are landfilled [15,19]. Because CDD has historically been considered relatively inert, a number of CDD landfills are unlined and do not include groundwater monitoring systems [16,21]. Given the presence of unencapsulated stockpiles, unlined landfills, and land applied recovered materials, understanding the leaching risks associated with PFAS in CDD grows increasingly important.

Existing studies have found PFAS concentrations in CDD landfill leachate ranging from 270 to 30,500 ng/L, comparable to those observed in MSW landfills [22]. These concentrations have been attributed to CDD materials like carpeting, stain resistant additives, and resins; however, while current research provides valuable insights on PFAS in various materials and consumer products stream [23-27], comprehensive examination of the CDD waste stream is lacking. Given the substantial volume of CDD generated and the potential for PFAS migration into the environment through CDD management practices (i.e., unlined landfills, leachate management, and recycling), there is a need to conduct an inventory of PFAS within CDD to assess material-specific risks. This study aimed to address gaps in the literature as highlighted by a recent study on landfilled PFAS, which identified that most data on this subject is limited to CDD landfill leachate and not the CDD waste stream itself [28].

Here, ten major categories of CDD —crushed concrete, mixed wood, asphalt shingles, gypsum drywall, carpet/foam padding, carpet, CDD fines, metals, cardboard, and reclaimed asphalt pavement (RAP)— were segregated by a CDD processing facility, representatively sampled, then characterized for total available PFAS. The same categories were then leached using two methodologies to evaluate the leaching potential associated with each material. Elevated PFAS concentrations in mixed wood components warranted further testing of wood subcategories to identify major contributing products. The total available and leachable PFAS data was then extrapolated using existing CDD inventories to approximate a national PFAS mass load from CDD. This study informs CDD managers and stakeholders of PFAS-relevant materials, the potential for PFAS to leach from these materials, and demonstrates the PFAS mass flow through current management pathways, providing the fundamental data needed to promote sustainable practices within the industry.

2. Materials and methods

2.1. Sample collection

Major CDD components were collected from a CDD MRF located in northern Florida. The facility processes around 5000 tons of CDD from commercial and residential sources from surrounding counties each month. The substantial throughput underscores the facility's broad service area and significant role in regional waste management. Nine categories of materials were collected on site, including crushed concrete, mixed wood, asphalt shingles, gypsum drywall, carpet padding, carpet, CDD fines, metal debris, and cardboard; however, because the facility did not process asphalt, RAP was collected from five stockpiling facilities across the state. A facility schematic that illustrates the material generation points and a description of components is provided in Fig. 1. The concrete is crushed with bricks and small amounts of tiles and granite. Clean wood products and yard trimmings are shredded to create mixed wood chips. Given the diversity of wood products within the mixed wood category, four major components of mixed wood were identified and collected on the site to better understand the distribution of PFAS within the category: oriented strand board (OSB), dimensional lumber, plywood, and yard trimmings. Additionally, since mixed wood was further processed into mulch, samples of the mulch were also collected. Materials that pass through the screening devices are categorized as CDD fines (< ¾ inch). These fines are mainly composed of soil, along with small fragments of wood, drywall, and concrete [29]. Constituting a significant portion of the total material, often exceeding 20% of the mass, CDD fines have the potential for beneficial reuse, such as serving as soil substitutes in construction fills or landfill covers [30]. However, they also present potential risks due to the presence of both organic and inorganic pollutants (Burdier et al., 2022).

While there are unavoidable limitations associated with sampling from a single facility, the facility's large intake and diverse sources help to enhance the representativeness of our samples. Careful measures were also implemented to reflect the variety and volume of CDD processed. To ensure representative sample collection across the major components of the CDD waste stream (concrete, mixed wood, cardboard, carpet padding, CDD fines, metal debris and RAP) samples were collected from multiple stockpiles containing material accumulated over several weeks. Samples were obtained from at least five sides of each stockpile at three distinct locations (top, middle, bottom). The rest of the collected materials (asphalt shingles, gypsum drywall and carpet) were generated on the sampling day and sampled in the same manner from a single stockpile. Samples were collected using stainless steel shovels which were methanol-rinsed prior to sampling and between collection of different categories to avoid contamination. All samples were placed in 19 L HDPE buckets and stored at 20 °C for no longer than 30 days before extraction. While the study provides valuable insights into PFAS concentrations at a major regional facility, the findings might not be directly applicable to other regions or facilities with different waste profiles.

2.2. Sample preparation and extraction

Representative subsamples from each component, except metal debris, were size reduced using methanol-rinsed tools. Due to the difficulty of metal size reduction, metals were tested in the state in which they were collected. Two different size reduction methods were used, tailored to the specific material being processed. Asphalt shingles,

cardboard, carpet, and carpet padding were first cut into 10 to 20 mm pieces and homogenized for further analysis. Crushed concrete, CDD fines, mixed wood chips, and RAP from each stockpile were thoroughly homogenized on separate methanol-rinsed polypropylene sheets following the American Society for Testing and Materials (ASTM) coning and quartering method to obtain representative subsamples (ASTM C702/C702M-11). A composite RAP sample was produced by combining equal masses of subsamples from the five locations sampled. All materials mentioned above were further pulverized with a methanol-rinsed blender to less than 4.75 mm when necessary, then 500–1000 g of size reduced material was collected for analysis.

In this study, we applied distinct extraction methods optimized for different sample matrices to ensure effective quantification of PFAS. Solvent extraction was used for solids, while solid-phase extraction was used for liquids. Extraction and analysis of total available PFAS in solids was adjusted from Ahmadireskety et al. [31]. Depending on the density of each material, between 1–5 g of size-reduced solid sample was placed into a 50 mL polypropylene tube and spiked with 30 μL isotopically labeled PFAS standards mixture (see Table S-1 in the SI). Ammonium hydroxide in methanol (0.3%) was added into each tube at a liquid to solid ratio (L/S) of 2. The solid and solvent mixture was vortexed for 1 min, sonicated for 30 min, rotated end-over-end for 30 min, then centrifuged at 4000 rpm for 20 min. Supernatants were transferred using a pipette, then the extraction process was repeated. The combined extracts were cleaned using 50 ± 5 mg of ENVI-Carb (Supelco) and evaporated to 1 mL using a nitrogen evaporator at 35 °C. Total PFAS analyses were performed in triplicate for each material.

To comprehensively assess leaching, two leaching protocols were used: leaching with nanopure water at a L/S of 10 and the USEPA Toxic Characteristics Leaching Procedure (TCLP), which was administered at an L/S of 20. Both leaching tests were performed on each major CDD category except for metal debris (due to the difficulty of size reducing this material to meet TCLP method requirements), where only nanopure water leaching was performed. During both leaching tests, materials were rotated end-over-end for a prescribed duration — 72 h for nanopure water leaching and 18 h for TCLP. After rotation, the solid-liquid mixture was centrifuged at 4000 rpm for 20 min and the supernatant leachates were transferred into HDPE bottles and stored at − 20 °C until PFAS extraction.

Leachates obtained from leaching tests were extracted using the solid-phase extraction protocol described in Liu et al. [9]. In brief, samples were pH-adjusted to between 4 and 5 with glacial acetic acid and spiked with 30 μL isotopically labeled PFAS standards mixture (see Table S-1). Phenomenex Strata-X-AW polymeric weak anion exchange cartridges (500 mg/6 mL) were conditioned with 0.3% ammonium hydroxide in methanol (4 mL), methanol (3 mL), and ammonium acetate/acetic acid buffer solution (4 mL, pH =4). The cartridges were washed with the buffer solution (4 mL) after sample loading and eluted with methanol (2 mL) and 0.3% ammonium hydroxide in methanol (2 ×3 mL). The eluted extracts were evaporated to 1 mL using a nitrogen evaporator at 35 °C. Each leaching test was performed in duplicate.

2.3. PFAS analysis

All extracts were analyzed and quantified for 92 PFAS via isotope dilution, using a Thermo Scientific Vanquish ultrahigh-pressure liquid chromatograph coupled to a TSQ Quantis triple quadrupole mass spectrometer (UHPLC-MS/MS). Only compounds detected in all replicates were reported using the average concentration in ng/g. Details regarding the reagents used and target PFAS abbreviations, chemical formulae, and corresponding isotopically labeled standards used for quantitation are summarized in Table S-1. The methodological limits of detection (LOD) and limits of quantification (LOQ) were defined as the peak area of analyte that yielded a signal-to-noise ratio of 3 and 10, respectively (see Table S-3). Only the PFAS detected above the LOQ across all replicate samples were reported to ensure accuracy. See the SI and Table S-2 for additional information regarding instrument operational conditions.

Quality control (QC) samples were utilized to validate the PFAS extraction and analysis method, which included extraction blanks, solvent blanks, and laboratory control samples; detailed information is available in the SI. Concentrations of all PFAS in extraction and solvent blanks were below the LOQ. For most detected PFAS, extraction efficiencies are above 70% in solids and liquids, with an average higher than 75%. Detailed QC results are provided in SI Table S4.

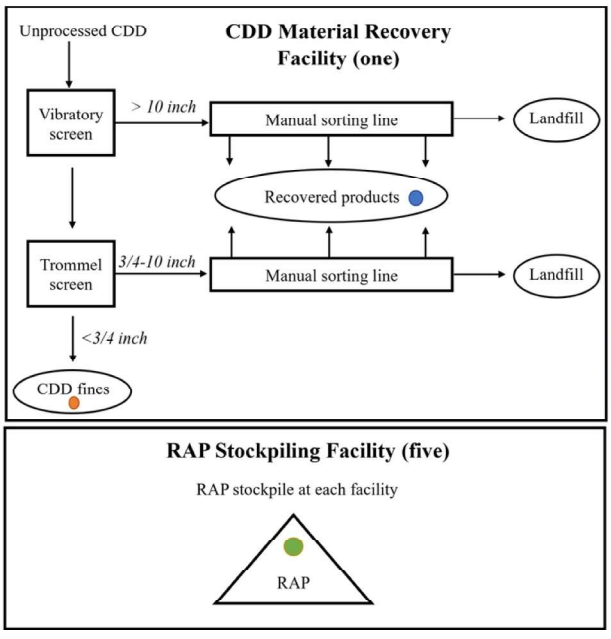

Category	Description
Concrete	Crushed concrete mixed with small amounts of bricks, tiles and granite
Mixed wood	Shredded mixed wood products including dimensional lumber, OSB, plywood, particle board, other non-treated wood products, and yard waste
Dimensional lumber	Wood fiber cut to a specific size
Plywood	A type of engineered wood
Oriented strand board	A type of engineered wood
Yard trimmings	Branches, leaves, flowers, trees
Mulch	Dyed mulch from shredded wood products, mainly from shredded dimensional lumber
Asphalt shingles	Roofing shingles used for waterproofing
Gypsum	Gypsum drywall used in the construction of interior walls and ceilings
Carpet/foam padding	Material placed underneath the carpet
Carpet	Textile floor covering
CDD fines	Fines fractions passed through processing facility screens
Metal debris	Mixed metal scraps (ferrous and non-ferrous metal)
Cardboard	Corrugated paper product
Reclaimed asphalt pavement	Milled asphalt/aggregate

Fig. 1. The layout of the CDD processing facility sampled and categories collected.

3. Results and discussion

3.1. Total available PFAS distribution in different CDD

In this work, nine major CDD materials were analyzed for total available PFAS. All tested materials contained at least one detectable compound, with the highest number of compounds detected in CDD fines (25 compounds) and the lowest in RAP (2 compounds). Total concentrations of the 92 PFAS measured, referred to as $\sum_{92}$PFAS hereafter, ranged from 1.0 ng/g for RAP to 190 ng/g for carpet. The $\sum_{92}$PFAS concentration broken down by PFAS subclass in each CDD material is presented in Fig. 2.

Of the materials tested, carpeting and carpet padding had the highest concentration of $\sum_{92}$PFAS at 190 ng/g and 170 ng/g, respectively, where perfluoroalkyl acid (PFAA)-precursors accounted for 99% and 85% of the $\sum_{92}$PFAS. Concentrations in these two categories were dominated by two precursors: N-ethylperfluorohexane sulfonamide (EtFHxSA) at 160 ng/g in carpet and 6:2 fluorotelomer sulfonate (6:2 FTS) at 110 ng/g in carpet padding and 21 ng/g in carpet. Levels of 6:2 FTS in carpets vary across studies. Some have reported non-detection of 6:2 FTS [32], whereas others have identified it at significantly higher levels compared to those found in our research [33]. These variations suggest that the levels of 6:2 FTS, and more generally, PFAS, can have wide variation depending on fabric treatment and carpet type. Notably, EtFHxSA has not been measured previously in carpeting, this being the first observation of its presence. Being by far the highest contributing compound found in carpet, these findings suggest a potential underestimation in PFAS from previous studies attributed to overlooked precursor compounds. In contrast to other studies, the only PFAAs detected in this study's carpet samples were PFOA and PFOS at 0.27 ng/g and 0.48 ng/g, respectively. Carpet paddings exhibited higher PFAAs concentrations, with PFOS being the most abundant at 7.3 ng/g. It is important to note that the specific types of carpet and carpet paddings were unknown in this study, with these findings highlighting the heterogeneity of CDD much like with MSW.

Gypsum drywall samples had the third highest total available $\sum_{92}$PFAS (120 ng/g). While PFAS in gypsum drywall have not been studied elsewhere, it is well-known that waterproofing additives have been added to commercial gypsum drywall to improve their performance in high moister environments (e.g., bathrooms, attics, or basements) [34,35]. Among the PFAS analyzed, 19 compounds were detected. Fluorotelomer phosphate diester (diPAPs) constituted the majority, accounting for 54% of $\sum_{92}$PFAS, with 6:2/8:2 diPAP and 8:2 diPAP being measured at 42 ng/g and 22 ng/g, respectively. Among the PFAAs identified, perfluorohexanoic acid (PFHxA) was the most abundant at 29 ng/g. PFHxA is commonly encountered as an impurity, a degradation product, or a metabolite originating from fluorotelomer-based products [31,36].

In the CDD fines, a substantial fraction of CDD often reused as soil replacement, 25 PFAS were detected with the total available $\sum_{92}$PFAS being 50 ng/g. The diversity of PFAS detected in CDD fines is likely due to the nature of processing, resulting in an accumulation of the fine fractions of all components, including but not limited to soil, small pieces of wood, concrete, brick, asphalt, and gypsum drywall [29]. PFAA-precursors were the dominant PFAS detected in CDD debris fines, representing 79% of $\sum_{92}$PFAS. Both 6:2 FTS and 6:2/8:2 diPAP were detected at the highest concentration of 14 ng/g. Three diPAPs (6:2diPAP, 6:2/8:2 diPAP and 8:2 diPAP) were detected in CDD debris fines with a total concentration of 21 ng/g. PFPeA was the highest detected PFCA (2.3 ng/g) and PFOS was the highest detected PFSA (1.3 ng/g). Interestingly, eight long chain PFCAs (C8-C16) and three long chain PFSAs (C6, C8, and C10) were all detected in CDD debris fines with a total concentration of 4.6 ng/g, making up 50% of PFAAs observed. This finding deviates from typical pattern reported in

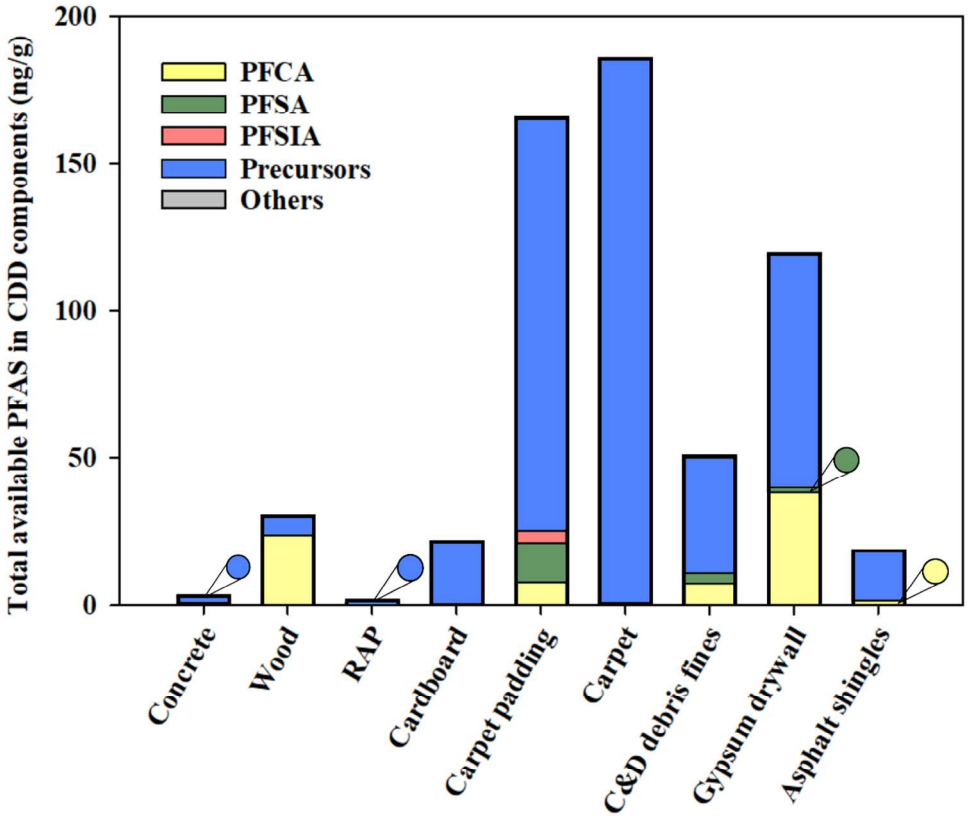

Fig. 2. Total available PFAS concentration in nine major CDD categories from a CDD processing facility. Metal debris was excluded from the total available PFAS analysis due to challenges with size reduction. Average values are reported for the three distinct triplicates analyzed for each material.

literature, where short chain PFAAs were the dominant PFAAs detected in environmental matrices such as indoor dust samples [37] due to the industry's shift from long chain to shorter chain PFAS [38].

In mixed wood samples, $\sum_{92}$PFAS was detected at 31 ng/g with the PFHxA had the highest concentration at 22 ng/g, consisting of 73% of $\sum_{92}$PFAS. Three precursors were also detected: 6:2 FTS at 5 ng/g, 6:2/8:2 diPAP at 1.1 ng/g, and diSAmPAP at 0.12 ng/g. Additionally, a novel PFAS, 7 H-perfluoroheptanoixc acid (7 H-PFHpA), was detected at 0.29 ng/g. Within the mixed wood category, OSB had the highest $\sum_{92}$PFAS at 380 ng/g, 13 times higher than that analyzed in mixed wood products. Plywood had the second highest $\sum_{92}$PFAS at 190 ng/g, followed by yard waste at 10 ng/g. The lowest $\sum_{92}$PFAS concentration was observed in dimensional lumber at 2.7 ng/g. Elevated PFAS levels in the two engineered wood products (OSB and plywood) align with findings from literature on PFAS use in engineered wood resigns [39]. Notably, PFCAs accounted for 97% of $\sum_{92}$PFAS in both OSB and plywood, with PFHxA detected at the highest concentration (360 and 180 ng/g, respectively), which is consistent with its prevalence in mixed wood samples. Potential sources of PFAS in yard waste could include the use of biosolids as fertilizer/soil amendment or yard sprays [40-42]. Mulch processed from mixed wood had $\sum_{92}$PFAS of 61 ng/g, twice of those observed in mixed wood itself, perhaps due to the water-resistant colorant or contamination during disposal and from the processing equipment used.

The remaining categories (RAP, concrete, cardboard, and asphalt shingles) had lower concentrations of PFAS ranging from 1.0 ng/g to 21 ng/g, with carboard having a similar concentration of diPAPs to other paper-based products such as toilet paper [43]. More details about the PFAS species detected and their concentrations within these materials are presented in Table S-5. PFAS were detected across all categories of material extracted. Some of these categories such as concrete, RAP, and metal debris had very small concentrations detected (close to 1 ng/g). It is theorized that the PFAS detected in these samples stem from contamination during the initial disposal phase, where these materials intermingle with other wastes containing elevated PFAS levels. Given that materials are received in a mixed state and subsequently sorted at the processing facility, pinpointing the exact origin of PFAS in these materials before disposal is challenging, highlighting the need for additional research. One approach to solve this issue could involve the collection and analysis of virgin materials that contribute to the CDD stream to ascertain baseline PFAS levels.

3.2. Leachable PFAS concentration in different CDD

Two leaching tests, nanopure water leaching and the TCLP, were employed to evaluate PFAS mobility in ten CDD debris categories. Each category was subjected to both leaching methods, except for metal debris, which were only processed with nanopure water leaching due to size reduction challenges. The pH for nanopure leaching ranged from 5 to 6, whereas for TCLP, it varied from 6 to 11 across different materials. Overall, the leaching behavior was consistent between the two leaching methods with the main difference being the concentrations observed, likely due to dilution (TCLP has twice the mass of leachate added than the nanopure method). This suggests that the presence of acetate had minimal impacts on the mobility of PFAS within these materials, as when normalized to the mass of PFAS released, both methods leached a similar mass of PFAS, within a variance of $\pm$ 10% across all material categories. This finding differs from those observed in soil studies where pH changes can significantly influence PFAS leachability [44,45]. This discrepancy can be attributed to the distinct physical and chemical properties between CDD and soil samples. Additionally, the dominant leachable PFAS found in CDD are short-chain PFCAs, which are less sensitive to solution pH even in soil [45]. Future studies should explore the impact of CDD properties and additional environmental factors such as temperature and water-soluble ions to enhance our understanding of PFAS mobility in CDD.

Results from nanopure water leaching, consistent with the TCLP leaching, are presented in Fig. 3 (detailed leachable concentrations from both leaching tests are displayed in Table S-6 and Table S-7). Across all categories the mass of PFAS which leached represented less than half the total available PFAS, meaning the majority of PFAS in CDD remained in the solid under the test conditions. This is notably lower than those reported in soil samples where similar L/S ratios and rotation times yielded an average leachability of 88–92% of the total available PFAS [46], suggesting the matrix have a significant impact on leaching behavior. The impact of matrix was also observed across different categories within the CDD components studied (Fig. 3B). For example, carpet and carpet padding, which despite having the highest levels of total available PFAS, leached less than 1% of their total PFAS content. In contrast, the materials which leached the most PFAS were not those with the highest overall content but rather those that had higher concentrations of PFCAs such as drywall, CDD fines, and mixed wood.

Overall, the leached concentrations from different components are lower than those observed in CDD landfills which were measured at an average of tens of thousands ng/L [22,47]. The differences could arise from the fact that landfills typically contain much less liquid relative to the amount of CDD than in a leaching test. For instance, typical landfills may have an L/S ratio of approximately 0.2 [48], whereas our tests were conducted at L/S ratios of 10 and 20. Additionally, the variety of other components received at CDD landfills, and the longer contact time between the materials and leachates could also play a role.

Although PFAAs-precursors made up the majority of the total available PFAS in most CDD components, PFAAs were the dominant PFAS detected in leachates from various materials under both leaching tests, representing up to 99% of leachable $\sum_{92}$PFAS. Among observed PFAAs, PFCAs were among the major congeners, particularly short chain PFCAs, comprised over 50% of leached PFAS in most components. This is likely due to the higher solubility of short chain PFAAs which partition to leachate relatively easily (Higgins et al., 2005; Yan et al., 2015). In addition to PFAAs, perfluorobutanesulfinic acid (referred to as Syn 34 in our methods in the SI), a perfluoroalkane sulfinic acid not previously reported in CDD, was detected at 0.039 and 0.066 ng/g in concrete, and 0.22 and 0.36 ng/g in carpet paddings under nanopure water leaching and TCLP, respectively. Among PFAAs-precursors analyzed, 6:2 FTS comprised almost all of the PFAAs-precursors in most CDD materials except in carpet and metal debris. In carpet, the predominant PFAA-precursor was EtFHxSA (around 50% by mass), which aligns with the previously noted abundance of this compound in carpet.

Overall, the leachability of PFAS appears to be dependent on the types of material as well as the PFAS present. It is well established that shorter chain PFAS (e.g., PFHxA) have a higher affinity for water and more easily leach than larger chain PFAS [49-51] so materials with these compounds, such as mixed wood or CDD fines, are more likely to readily leach PFAS. In contrast, materials like carpeting or carpet padding which are treated with long chain precursor PFAS for stain resistance, likely explaining why high concentrations of total PFAS were detected, while very few PFAS leached during batch tests. Furthermore, materials that lose structural integrity when saturated, such as gypsum drywall, likely contribute to the increased release of PFAS during leaching tests. Future research should investigate the leaching behavior of PFAS under simulated landfill conditions to determine if the materials which did not readily leach PFAS under batch conditions such as carpeting continue to be sinks or if they eventually degrade and begin to release PFAS after a certain timeframe.

3.3. National CDD PFAS load and disposal fate

As previously described, the concerns regarding PFAS in CDD management primarily stem from the unencapsulated nature of CDD disposal, recycling, and beneficial reuse. To determine the PFAS load distribution among different management pathways, the total available PFAS data generated in this study was extrapolated using existing US

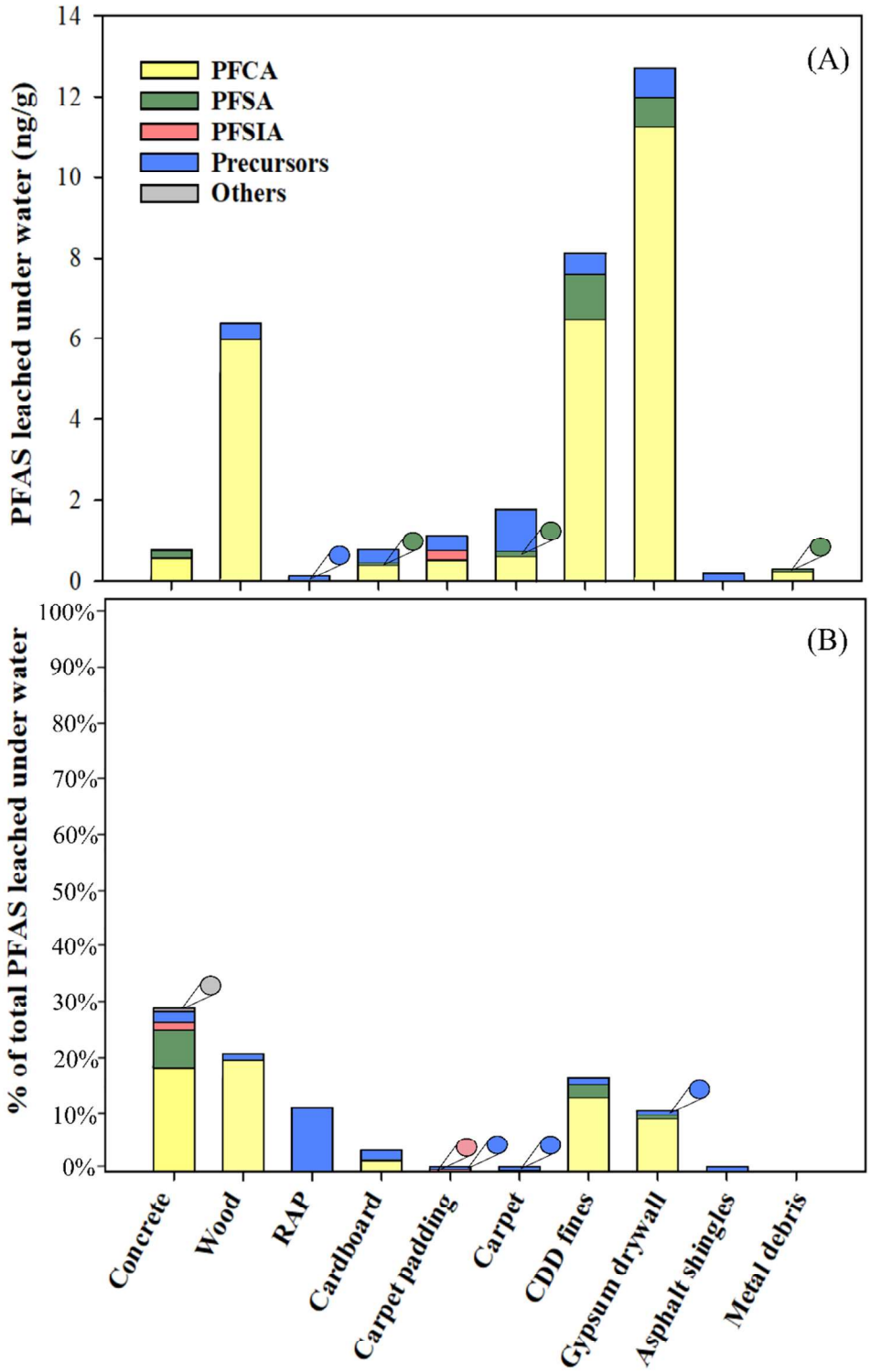

Fig. 3. Concentration of PFAS in leachate from the ten materials tested. (A) represents the nanopure water leaching results and includes metal debris; (B) represents percentage of the PFAS mass that leached relative to the total mass of PFAS available in that material, excluding metal debris due to absence of data on the total available PFAS. Reported averages in (A) are triplicates of aliquoted material extracted and in (B) are triplicates of three batch leaching tests.

generation and disposal statistics. First, an annual mass of CDD was calculated by assuming a per capita generation rate of 1.84 Mg CDD per year and multiplying by 2023 US census estimations [19,52,53]. The resulting 620 million metric tons of CDD was then scaled based on national generation, disposal, and recycling quantities for seven categories made available by the US EPA: concrete, wood, drywall, metal debris, brick/clay tile, asphalt shingles, and asphalt concrete [53]. Distinction between disposal into lined versus unlined landfills was assessed using survey data from a 2006 study on state specific CDD landfill liner requirements at the time [16]. Though some liner requirements have evolved since the publication of Clark et al. [16], it remains the most comprehensive assessment to date and serves as a valuable benchmark for our estimations. To accommodate for potential changes, we conservatively assumed that only states identified in Clark et al. [16]

having no liner requirements disposed all CDD to unlined landfills. Conversely, states with any form of liner requirements were assumed to employ lined landfills for CDD disposal. Finally, the material specific total PFAS concentrations from this study were applied to CDD management stages to estimate PFAS mass flow. Details and assumptions associated with this estimation are provided in Table S-8. Detailed equations used for the estimation are also displayed in the SI.

Fig. 4 illustrates the mass flow of PFAS in the US CDD waste stream with respect to disposal and recycling/reuse. It should be noted that these calculations do not represent exact PFAS masses but aim to provide relative comparisons between management sectors. From the 620 million metric tons of CDD, a total available PFAS mass of 4800 kg was estimated in the CDD stream (7.7 ng/g). The bulk of this mass originates from drywall/plaster, wood products, and concrete, accounting for 39%, 26%, and 26%, respectively. The remaining materials, shingles, asphalt concrete, brick/tile, and metal combined, accounted for 9%. Drywall/plaster and wood product contributions are attributed to high total PFAS concentrations in the materials themselves; however, contribution from concrete, one of the lowest concentrated materials, resulted from high generation quantities. As bulky materials like asphalt and concrete represent more than half of the total US CDD waste stream and can be derived from many applications (e.g., airport pavement, buildings, bridges), future studies should more comprehensively assess these materials to better understand their true impacts on PFAS management.

After generation most CDD (depending on the material) is recycled in the form of compost/mulch, manufactured products, aggregate, fuel, or soil amendment; only 24% being landfilled [53]. Despite this, when considering material-specific management, landfills disproportionately bear the total PFAS mass – 3000 kg compared to the 1800 kg diverted to recycling operations. Though a thorough, component-based assessment of total extractable PFAS in MSW has yet to be conducted, a review by Tolaymat et al. [28] reported an estimated 6600 kg of total available PFAS in the 150 million tons of MSW landfilled in 2018 – twice the amount estimated for landfilled CDD in this study. Although CDD generation in the US is double that of MSW, landfilled quantities are roughly similar (MSW~150 million tons, CDD~140 million tons) [53], suggesting generally higher concentrations of PFAS in the components of MSW, though more detailed research, especially considering the heterogeneous nature of MSW, is needed.

In the context of landfill management, the leachability of PFAS is of paramount concern as it represents the fraction that may migrate into landfill leachate. The percentage of PFAS leached from landfilled MSW and CDD components appears to be similar. Drawing from existing research, Tolaymat et al. [28] estimated 10% of PFAS from landfilled MSW to be leachable, comparable to the 12% determined for landfilled CDD in this study. Studies also reported comparable PFAS concentrations in leachates from lined CDD landfills and MSW landfills [22]. However, unlike MSW, one third of landfilled CDD is disposed of in unlined landfills according to Clark et al. [16] – a 4% (120 kg) annual release, directly to surrounding environments. More concerning, 4% should be viewed as a minimum possible release from CDD, as other categories with notable PFAS levels, such as CDD fines, were not accounted for and additional leaching from land applied CDD or CDD disposed of in minimally engineered landfills (e.g., natural clay liners) is not considered. Therefore, while MSW may be a higher PFAS-concentrated waste stream, the leaching risks posed by CDD are equally significant, if not weightier, due to generation quantities and lack of regulatory oversight in land application of recycled CDD materials and CDD liner controls.

4. Conclusions

This work provides a detailed analysis of total available and leachable PFAS concentrations in major CDD categories segregated by a CDD processing facility, a topic with limited information in the literature. We found substantial variations in $\sum_{92}$PFAS concentrations, ranging from 1 ng/g (RAP) to 190 ng/g (carpet), with a majority mass of the $\sum_{92}$PFAS detected coming from precursor species. Though on average the mass of PFAS from the totals analyses was dominated by PFAA-precursors, leachable PFAS consisted mainly of PFCAs, likely because of their higher solubility. Materials with high total PFAS concentrations, like carpets, exhibited minimal leaching (<1%), while more porous materials such as drywall showed higher leaching rates (between 7% to 14%).

This study extrapolated material-specific PFAS data to understand

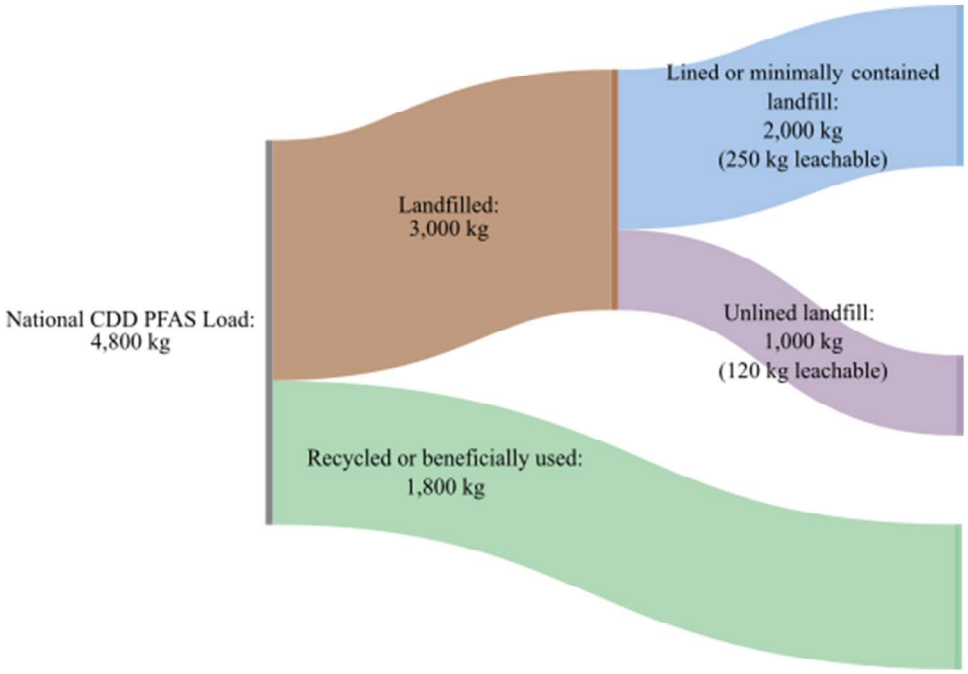

Fig. 4. Estimated total available PFAS mass flow though US CDD management stages extrapolated with findings from this study. Material-specific concentrations were applied to national CDD generation and composition, yielding an annual PFAS load from the waste stream, which was further evaluated using available data on CDD management.

the broader implications for CDD management in the US, estimating a total PFAS mass of 4800 kg within the 620 million metric tons of CDD waste. Drywall/plaster, wood products, and concrete were the main contributors, accounting for 39%, 26%, and 26% of the total PFAS mass, respectively. Despite most CDD being recycled or reused, landfills still accumulate significant PFAS mass (3000 kg) mainly from drywall and wood. Approximately 12% of the PFAS in CDD landfills could leach, a rate comparable to MSW (~10%) [28]. The presence of one third of landfilled CDD in unlined landfills raises concerns about direct leaching risks. These findings suggest that CDD, a larger and less regulated waste stream than MSW, may pose a similar, if not greater leaching risk.

While this study provides an initial overview, its extrapolations from a single CDD processing facility may not fully capture the variability across different locations, potential contamination from material commingling during disposal, or environmental factors that might impact PFAS mobility. These limitations underscore the need for comprehensive investigations to characterize PFAS in diverse CDD settings and virgin materials across various geographical areas, and to examine how environmental conditions influence PFAS mobility.

Environmental implication

This study underscores the environmental significance of PFAS in construction and demolition debris (CDD), a major waste stream with limited research and oversight. By identifying elevated concentrations of various PFAS, including precursors and terminal species in CDD materials, the study underscores the hazardous nature of these substances due to their persistence and potential for environmental release. Findings suggest that landfilled CDD may present similar, if not greater, leaching risks as municipal solid waste. This work advances understanding of PFAS distribution in CDD waste streams, informing effective management strategies and regulatory policies to mitigate environmental contamination and protect public health.

CRediT authorship contribution statement

Timothy Townsend: Writing – review & editing, Visualization, Supervision, Resources, Project administration, Funding acquisition, Data curation, Conceptualization. **Jake Thompson:** Writing – review & editing, Visualization, Validation, Formal analysis, Conceptualization. **John Bowden:** Writing – review & editing, Validation, Conceptualization. **Yalan Liu:** Writing – original draft, Visualization, Validation, Methodology, Investigation, Formal analysis, Data curation, Conceptualization. **Ashley Lin:** Writing – review & editing, Visualization, Validation, Formal analysis, Conceptualization.

Declaration of Competing Interest

The authors declare the following financial interests/personal relationships which may be considered as potential competing interests. Timothy Townsend reports financial support was provided by United States Environmental Protection Agency. If there are other authors, they declare that they have no known competing financial interests or personal relationships that could have appeared to influence the work reported in this paper.

Data availability

Data will be made available on request.

Acknowledgments

This work was supported by the U.S. Environmental Protection Agency (grant number 83962001–0). The authors thank the operators of the facilities involved in the study.

Appendix A. Supporting information

Supplementary data associated with this article can be found in the online version at doi:10.1016/j.jhazmat.2024.134567.

References

[1] Evich, M.G., Davis, M.J.B., McCord, J.P., Acrey, B., Awkerman, J.A., Knappe, D.R. U., Lindstrom, A.B., Speth, T.F., Tebes-Stevens, C., Strynar, M.J., Wang, Z., Weber, E.J., Henderson, W.M., Washington, J.W., 2022. Per- and polyfluoroalkyl substances in the environment. Science 375, eabg9065. https://doi.org/10.1126/science.abg9065.

[2] Fenton, S.E., Ducatman, A., Boobis, A., DeWitt, J.C., Lau, C., Ng, C., Smith, J.S., Roberts, S.M., 2021. Per- and Polyfluoroalkyl Substance Toxicity and Human Health Review: Current State of Knowledge and Strategies for Informing Future Research. Environ Toxicol Chem 40, 606–630. https://doi.org/10.1002/etc.4890.

[3] FDEP, 2019. Provisional Cleanup Target Levels for PFOA and PFOS in Groundwater and Soil | Florida Department of Environmental Protection. URL ⟨https://floridadep.gov/waste/district-business-support/documents/provisional-cleanup-target-levels-pfoa-and-pfos⟩ (accessed 1.27.22).

[4] MADEP, 2021. PFOA and PFOS, Maine Department of Environmental Protection. URL ⟨https://www1.maine.gov/dep/spills/topics/pfas/index.html⟩ (accessed 1.24.22).

[5] U.S. EPA, 2022. Resident Soil to Groundwater RSLs Table. URL ⟨https://semspub.epa.gov/work/HQ/402393.pdf⟩ (accessed 5.20.22).

[6] Benskin, J.P., Li, B., Ikonomou, M.G., Grace, J.R., Li, L.Y., 2012. Per- and Polyfluoroalkyl Substances in Landfill Leachate: Patterns, Time Trends, and Sources. Environ Sci Technol 46, 11532–11540. https://doi.org/10.1021/es302471n.

[7] Chen, Y., Zhang, H., Liu, Y., Bowden, J.A., Tolaymat, T.M., Townsend, T.G., Solo-Gabriele, H.M., 2023. Evaluation of per- and polyfluoroalkyl substances (PFAS) in leachate, gas condensate, stormwater and groundwater at landfills. Chemosphere 318, 137903. https://doi.org/10.1016/j.chemosphere.2023.137903.

[8] Lang, J.R., Allred, B.M., Field, J.A., Levis, J.W., Barlaz, M.A., 2017. National Estimate of Per- and Polyfluoroalkyl Substance (PFAS) Release to U.S. Municipal Landfill Leachate. Environ Sci Technol 51, 2197–2205. https://doi.org/10.1021/acs.est.6b05005.

[9] Liu, Y., Robey, N.M., Bowden, J.A., Tolaymat, T.M., da Silva, B.F., Solo-Gabriele, H.M., Townsend, T.G., 2021. From Waste Collection Vehicles to Landfills: Indication of Per- and Polyfluoroalkyl Substance (PFAS) Transformation. Environ Sci Technol Lett 8, 66–72. https://doi.org/10.1021/acs.estlett.0c00819.

[10] Wang, N., Liu, J., Buck, R.C., Korzeniowski, S.H., Wolstenholme, B.W., Folsom, P. W., Sulecki, L.M., 2011. 6:2 fluorotelomer sulfonate aerobic biotransformation in activated sludge of waste water treatment plants. Chemosphere 82, 853–858. https://doi.org/10.1016/j.chemosphere.2010.11.003.

[11] Yan, H., Zhang, C.-J., Zhou, Q., Chen, L., Meng, X.-Z., 2012. Short- and long-chain perfluorinated acids in sewage sludge from Shanghai, China. Chemosphere 88, 1300–1305. https://doi.org/10.1016/j.chemosphere.2012.03.105.

[12] Zhou, T., Li, X., Liu, H., Dong, S., Zhang, Z., Wang, Z., Li, J., Nghiem, L.D., Khan, S. J., Wang, Q., 2024. Occurrence, fate, and remediation for per-and polyfluoroalkyl substances (PFAS) in sewage sludge: A comprehensive review. J Hazard Mater 466, 133637. https://doi.org/10.1016/j.jhazmat.2024.133637.

[13] Glenn, G., Shogren, R., Jin, X., Orts, W., Hart-Cooper, W., Olson, L., 2021. Per- and polyfluoroalkyl substances and their alternatives in paper food packaging. Compr Rev Food Sci Food Saf 20, 2596–2625. https://doi.org/10.1111/1541-4337.12726.

[14] Trier, X., Taxvig, C., Rosenmai, A.K., Pedersen, G.A., 2018. PFAS in paper and board for food contact: Options for risk management of poly- and perfluorinated substances. Nordic Council of Ministers,.

[15] US EPA, O., 2017. Construction and Demolition Debris: Material-Specific Data. URL ⟨https://www.epa.gov/facts-and-figures-about-materials-waste-and-recycling/construction-and-demolition-debris-material⟩ (accessed 12.12.23).

[16] Clark, C., Jambeck, J., Townsend, T., 2006. A review of construction and demolition debris regulations in the United States. Crit Rev Environ Sci Technol 36, 141–186. https://doi.org/10.1080/10643380500531197.

[17] Cochran, K., Townsend, T., Reinhart, D., Heck, H., 2007. Estimation of regional building-related C&D debris generation and composition: Case study for Florida, US. Waste Manag 27, 921–931. https://doi.org/10.1016/j.wasman.2006.03.023.

[18] Yeheyis, M., Hewage, K., Alam, M.S., Eskicioglu, C., Sadiq, R., 2013. An overview of construction and demolition waste management in Canada: a lifecycle analysis approach to sustainability. Clean Technol Environ Policy 15, 81–91. https://doi.org/10.1007/s10098-012-0481-6.

[19] Townsend, T.G., Anshassi, M., 2023. Construction and Demolition Debris, Waste Management Principles and Practice. Springer International Publishing,, Cham. https://doi.org/10.1007/978-3-031-25013-2.

[20] Lin, A.M., Timshina, A.S., Magnuson, J.K., Bowden, J.A., Townsend, T.G., 2023. Emerging polycyclic aromatic hydrocarbon (PAH) and trace metal leachability from reclaimed asphalt pavement (RAP). Chemosphere 333, 138937. https://doi.org/10.1016/j.chemosphere.2023.138937.

[21] Powell, J.T., Jain, P., Smith, J., Townsend, T.G., Tolaymat, T.M., 2015. Does Disposing of Construction and Demolition Debris in Unlined Landfills Impact Groundwater Quality? Evidence from 91 Landfill Sites in Florida. Environ Sci Technol 49, 9029–9036. https://doi.org/10.1021/acs.est.5b01368.

[22] Solo-Gabriele, H.M., Jones, A.S., Lindstrom, A.B., Lang, J.R., 2020. Waste type, incineration, and aeration are associated with per- and polyfluoroalkyl levels in landfill leachates. Waste Manag 107, 191–200. https://doi.org/10.1016/j.wasman.2020.03.034.
[23] Bečanová, J., Melymuk, L., Vojta, Š., Komprdová, K., Klánová, J., 2016. Screening for perfluoroalkyl acids in consumer products, building materials and wastes. Chemosphere 164, 322–329. https://doi.org/10.1016/j.chemosphere.2016.08.112.
[24] Glüge, J., Scheringer, M., Cousins, I.T., DeWitt, J.C., Goldenman, G., Herzke, D., Lohmann, R., Ng, C.A., Trier, X., Wang, Z., 2020. An overview of the uses of per- and polyfluoroalkyl substances (PFAS). Environ Sci Process Impacts 22, 2345–2373. https://doi.org/10.1039/D0EM00291G.
[25] Janousek, R.M., Lebertz, S., Knepper, T.P., 2019. Previously unidentified sources of perfluoroalkyl and polyfluoroalkyl substances from building materials and industrial fabrics. Environ Sci Process Impacts 21, 1936–1945. https://doi.org/10.1039/C9EM00091G.
[26] Sanborn Head, 2019. PFAS WASTE SOURCE TESTING REPORT. URL ⟨https://anrweb.vt.gov/PubDocs/DEC/SolidWaste/OL510/OL510%202019.10.15%20NEWSVT%20PFAS%20Source%20Testing%20Rpt%20-%20Final.pdf⟩ (accessed 1.18.24).
[27] Wu, Y., Romanak, K., Bruton, T., Blum, A., Venier, M., 2020. Per- and polyfluoroalkyl substances in paired dust and carpets from childcare centers. Chemosphere 251, 126771. https://doi.org/10.1016/j.chemosphere.2020.126771.
[28] Tolaymat, T., Robey, N., Krause, M., Larson, J., Weitz, K., Parvathikar, S., Phelps, L., Linak, W., Burden, S., Speth, T., Krug, J., 2023. A critical review of perfluoroalkyl and polyfluoroalkyl substances (PFAS) landfill disposal in the United States. Sci Total Environ 905, 167185. https://doi.org/10.1016/j.scitotenv.2023.167185.
[29] Townsend, T., Tolaymat, T., Leo, K., Jambeck, J., 2004. Heavy metals in recovered fines from construction and demolition debris recycling facilities in Florida. Sci Total Environ 332, 1–11. https://doi.org/10.1016/j.scitotenv.2004.03.011.
[30] Su, J., Laux, S.J., Townsend, T.G., 2018. Trace chemical partitioning in construction and demolition debris fines: process and market implications. J Mater Cycles Waste Manag 20, 1416–1427. https://doi.org/10.1007/s10163-018-0700-2.
[31] Ahmadireskety, A., Da Silva, B.F., Townsend, T.G., Yost, R.A., Solo-Gabriele, H.M., Bowden, J.A., 2021. Evaluation of extraction workflows for quantitative analysis of per- and polyfluoroalkyl substances: A case study using soil adjacent to a landfill. Sci Total Environ 760, 143944. https://doi.org/10.1016/j.scitotenv.2020.143944.
[32] Zheng, G., Boor, B.E., Schreder, E., Salamova, A., 2020. Indoor exposure to per- and polyfluoroalkyl substances (PFAS) in the childcare environment. Environ Pollut 258, 113714. https://doi.org/10.1016/j.envpol.2019.113714.
[33] Wu, Y., Romanak, K., Bruton, T., Blum, A., Venier, M., 2020. Per- and polyfluoroalkyl substances in paired dust and carpets from childcare centers. Chemosphere 251, 126771. https://doi.org/10.1016/j.chemosphere.2020.126771.
[34] Alfawakhiri, F., Sultan, M.A., MacKinnon, D.H., 1999. Fire resistance of loadbearing steel-stud wall protected with gypsum board: a review. Fire Technol 35, 308–335. https://doi.org/10.1023/A:1015401029995.
[35] Li, Z., Xu, K., Peng, J., Wang, J., Zhang, J., Li, Q., 2021. Study on mechanical strength and water resistance of organosilicon waterproofing agent blended recycled gypsum plaster. Case Stud Constr Mater 14, e00546. https://doi.org/10.1016/j.cscm.2021.e00546.
[36] Luz, A.L., Anderson, J.K., Goodrum, P., Durda, J., 2019. Perfluorohexanoic acid toxicity, part I: Development of a chronic human health toxicity value for use in risk assessment. Regul Toxicol Pharmacol 103, 41–55. https://doi.org/10.1016/j.yrtph.2019.01.019.
[37] Ao, J., Yuan, T., Xia, H., Ma, Y., Shen, Z., Shi, R., Tian, Y., Zhang, J., Ding, W., Gao, L., Zhao, X., Yu, X., 2019. Characteristic and human exposure risk assessment of per- and polyfluoroalkyl substances: A study based on indoor dust and drinking water in China. Environ Pollut 254, 112873. https://doi.org/10.1016/j.envpol.2019.07.041.
[38] Karásková, P., Venier, M., Melymuk, L., Bečanová, J., Vojta, Š., Prokeš, R., Diamond, M.L., Klánová, J., 2016. Perfluorinated alkyl substances (PFASs) in household dust in Central Europe and North America. Environ Int 94, 315–324. https://doi.org/10.1016/j.envint.2016.05.031.
[39] Glüge, J., Scheringer, M., Cousins, T., I., C, DeWitt, J., Goldenman, G., Herzke, D., Lohmann, R., A. Ng, C., Trier, X., Wang, Z., 2020. An overview of the uses of per- and polyfluoroalkyl substances (PFAS). Environ Sci Process Impacts 22, 2345–2373. https://doi.org/10.1039/D0EM00291G.
[40] Brunn, H., Arnold, G., Körner, W., Rippen, G., Steinhäuser, K.G., Valentin, I., 2023. PFAS: forever chemicals—persistent, bioaccumulative and mobile. Reviewing the status and the need for their phase out and remediation of contaminated sites. Environ Sci Eur 35, 20. https://doi.org/10.1186/s12302-023-00721-8.
[41] Johnson, G.R., 2022. PFAS in soil and groundwater following historical land application of biosolids. Water Res 211, 118035. https://doi.org/10.1016/j.watres.2021.118035.
[42] Thompson, J.T., Robey, N.M., Tolaymat, T.M., Bowden, J.A., Solo-Gabriele, H.M., Townsend, T.G., 2023. Underestimation of Per- and Polyfluoroalkyl Substances in Biosolids: Precursor Transformation During Conventional Treatment. Environ Sci Technol. https://doi.org/10.1021/acs.est.2c06189.
[43] Thompson, J.T., Chen, B., Bowden, J.A., Townsend, T.G., 2023. Per- and Polyfluoroalkyl Substances in Toilet Paper and the Impact on Wastewater Systems. Environ Sci Technol Lett 10, 234–239. https://doi.org/10.1021/acs.estlett.3c00094.
[44] Li, Y., Oliver, D.P., Kookana, R.S., 2018. A critical analysis of published data to discern the role of soil and sediment properties in determining sorption of per and polyfluoroalkyl substances (PFASs). Sci Total Environ 628–629, 110–120. https://doi.org/10.1016/j.scitotenv.2018.01.167.
[45] Nguyen, T.M.H., Bräunig, J., Thompson, K., Thompson, J., Kabiri, S., Navarro, D. A., Kookana, R.S., Grimison, C., Barnes, C.M., Higgins, C.P., McLaughlin, M.J., Mueller, J.F., 2020. Influences of Chemical Properties, Soil Properties, and Solution pH on Soil–Water Partitioning Coefficients of Per- and Polyfluoroalkyl Substances (PFASs). Environ Sci Technol 54, 15883–15892. https://doi.org/10.1021/acs.est.0c05705.
[46] Rayner, J.L., Slee, D., Falvey, S., Kookana, R., Bekele, E., Stevenson, G., Lee, A., Davis, G.B., 2022. Laboratory batch representation of PFAS leaching from aged field soils: Intercomparison across new and standard approaches. Sci Total Environ 838, 156562. https://doi.org/10.1016/j.scitotenv.2022.156562.
[47] Chen, Y., Zhang, H., Liu, Y., Bowden, J.A., Tolaymat, T.M., Townsend, T.G., Solo-Gabriele, H.M., 2022. Concentrations of perfluoroalkyl and polyfluoroalkyl substances before and after full-scale landfill leachate treatment. Waste Manag 153, 110–120.
[48] Liu, Y., Mendoza-Perilla, P., Clavier, K.A., Tolaymat, T.M., Bowden, J.A., Solo-Gabriele, H.M., Townsend, T.G., 2022. Municipal solid waste incineration (MSWI) ash co-disposal: Influence on per- and polyfluoroalkyl substances (PFAS) concentration in landfill leachate. Waste Manag 144, 49–56. https://doi.org/10.1016/j.wasman.2022.03.009.
[49] Gellrich, V., Stahl, T., Knepper, T.P., 2012. Behavior of perfluorinated compounds in soils during leaching experiments. Chemosphere 87, 1052–1056. https://doi.org/10.1016/j.chemosphere.2012.02.011.
[50] Higgins, C.P., Luthy, R.G., 2006. Sorption of Perfluorinated Surfactants on Sediments. Environ Sci Technol 40, 7251–7256. https://doi.org/10.1021/es061000n.
[51] Kabiri, S., Tucker, W., Navarro, D.A., Bräunig, J., Thompson, K., Knight, E.R., Nguyen, T.M.H., Grimison, C., Barnes, C.M., Higgins, C.P., Mueller, J.F., Kookana, R.S., McLaughlin, M.J., 2022. Comparing the leaching behavior of per- and polyfluoroalkyl substances from contaminated soils using static and column leaching tests. Environ Sci Technol 56, 368–378. https://doi.org/10.1021/acs.est.1c06604.
[52] US Census Bureau, 2020. State Population Totals and Components of Change: 2020–2023.
[53] US EPA, 2020. Advancing Sustainable Materials Management: 2018 Fact Sheet.

Supporting Information for:

Per- and Polyfluoroalkyl Substances (PFAS) in Construction and Demolition Debris: Discerning Sources and Fate During Management

Yalan Liu[1,2], Ashley Lin[2], Jake Thompson, John Bowden[2,3], Timothy G Townsend[2]*,

[1]Department of Civil, Environmental and Geomatics Engineering, Florida Atlantic University, Boca Raton, FL, USA 33431

[2]Department of Environmental Engineering Sciences, University of Florida; PO Box 116450, Gainesville, FL, USA 32611-6450

[2]Department of Department of Physiological Sciences, University of Florida; Gainesville, Florida, 1333 Center Drive, Basic Science Building, Room 324, Gainesville, FL, USA 32610

Submitted to:

Journal of Hazardous Materials

*Corresponding author. Phone: 352-392-0846; Email: ttown@ufl.edu

Title	**Page**
Sample and Data Analysis	S3
Quality Control and Interpretation	S4
Table S-1. Lists of native PFAS and corresponding IS for quantification.	S6
Table S-2. LC-MS/MS operation conditions	S10
Table S-3. Compound-specific method LOD and LOQ	S11
Table S-4. Extraction efficiency results for detected PFAS in solids and liquids	S14
Table S-5. Total available PFAS concentrations detected in nine major CDD waste.	S15
Table S-6. Leachable PFAS detected using nanopure water leaching test.	S17
Table S-7. Leachable PFAS detected using TCLP	S19
Table S-8. Data and corresponding sources utilized for national CDD extrapolation	S21

Supplemental Materials

Sample and Data Analysis

Water, methanol, acetonitrile, ammonium hydroxide, ammonium acetate and formic acid (all Optima grade) were purchased from Thermo Fisher Scientific (Waltham, MA, USA). All standards (6 native and 6 mass-labeled) were purchased from Wellington Laboratories (Guelph, ON, Canada) or were donated by Synquest Laboratories or Oakwood Chemicals. Standards and their abbreviations can be found in Table S-1. Soil and leachate extracts were analyzed via targeted ultra-high pressure liquid chromatography-tandem mass spectrometry (UHPLC-MS/MS) using a Thermo Vanquish UHPLC system (Waltham, MA, USA) coupled to a Thermo Quantis triple quadrupole mass spectrometer (operated with electrospray in negative ionization mode and scanning via scheduled selected reaction monitoring (SRM)).

A Gemini C18 (100 x 2 mm; 3µm) column from Phenomenex was used for chromatographic separation. Water [A] and methanol [B] both containing 5 mM of ammonium acetate were used as the mobile phase. The gradient elution was set as 0-3 min 10% B, 3-4.5 min 10-35% B, 4.5-12.5 min 35-95% B, 12.5-12.51 min 95-99 % B, 12.51-19 min 99%, and then equilibrated to initial conditions in 30 min. The temperature of the autosampler was 4 °C, the flow rate was 0.5 mL min^{-1}, and injection volume was 10 µL. Water, methanol, and ammonium acetate used in the study were all Optimal grade purchased from Fisher Scientific. Scheduled SRM mode (monitoring two transitions, if possible) was used to detect and quantify each PFAS (mass-labeled species are shown in Tables S-1). The most intense transition was used for quantification, while the second transition was used to confirm identification (if applicable). For PFAS where no isotopically-labeled standard was available, an alternative labeled standard, either similar by

structure or retention time, was selected for quantitation. Table S-2 displays additional LC-MS/MS parameters.

Target PFAS in this study included: 10 perfluoroalkyl sulfonic acids (PFSAs) (C3-C10, C12); 22 per- and polyfluoroalkyl carboxylic acids (PFCAs) (C4-C14, C16, C18, P4MOA, Syn 46 (unsaturated PFCA), Oak 8 (perfluoroalkyl dioic acid), Syn 43 (perfluoroalkyl dioic acid), Syn 45 (perfluoroalkyl dioic acid), Syn 28 (H-substituted PFCA), Syn 35, Oak 10 (H-substituted PFCA), Oak 6 (H-substituted PFCA)); 1 perfluoroalkyl phosphonic acid (PFPA) (C6); 1 perfluoroalkyl sulfinic acid (PFSiA) (C4); 11 Per- and polyfluoroether carboxylic acids (PFECAs) (HFPO-DA (commercial name GenX), HFPO-TA (Syn 68), HFPO-TeA (Syn 59), NaDONA, Syn 62 (H-substituted PFECA), Syn 53, Syn 38, Syn 71, Oak 37, PF4OPeA, 3,6-OPFHpA; 5 Perfluoroether sulfonic acids (PFESAs) (PFEESA, Syn 72, Syn 32, 11 Cl-PF3OUDS, 9Cl-PF3ONS); 42 perfluoroalkyl acid (PFAA) precursors including n:2 fluorotelomer sulfonic acids (n:2 FTS) (4:2, 6:2, 8:2 and 10:2 FTS; n:2 fluorotelomer carboxylic acids (n:2 FTCAs) (6:2, 8:2, and 10:2 FTCA also known as FHEA, FOEA, FDEA, respectively); n:3 FTCA (3:3, 5:3, 7:3FTCA also known as FPrPA, FPePA, FHpPA, respectively, and oak 9 (6:3 FTCA), and Syn 58 (8:3 FTCA); n:2 unsaturated fluorotelomer carboxylic acids (n:2 FTUCA) (6:2, 8:2 and 10:2 FTUCA also known as FHUEA, FOUEA, and FDUEA, respectively); perfluoroalkyl phosphinic acids (PFPi) (6:6 and 6:8 PFPi); polyfluoroalkyl phosphate diesters (diPAPs) (6:2, 8:2 and 6:2/8:2 diPAP; diSAmPAP); perfluoroalkane sulfonamides (FASA) (FBSA; MeFBSA; FHxSA; N-AP-FHxSA; N-TAmP-FHxSA; N-CMAmP-6:2FOSA (6:2 FTAB); FOSA; FDSA; N-MeFOSA; N-EtFOSA); perfluoroalkane sulfonamido acetic acids (FASAAs) (FOSAA; N-MeFOSAA; N-EtFOSAA, Syn 5); perfluoroalkane sulfonamidoethanols (FASEs) (Syn 2, Oak 36); fluorotelomer alcohols (FTOHs) (5:2 FTOH; 7:2 FTOH), and three other PFAS: 8Cl-PFOS, PFECHS, and Syn 12. Details

about the targeted PFAS abbreviation, chemical formula, and the corresponding IS used for quantification is summarized in the Table S-1.

Quality Control and Interpretation

Three quality control (QC) sample types were analyzed in parallel with both leachate and solid samples: (1) method blanks, (2) solvent blanks, (3) matrix matched quality control samples.

Method blanks were created using 15 ml of optima water in 50 ml falcon tubes and extracted with every batch of unknown samples. They were used to confirm that no PFAS was introduced during sample preparation and extraction. Within the mass spectrometric batch queue, for sample injection, a solvent blank (made of optima methanol) was run between each sample to exclude and monitor any potential carryover effects. Matrix matched quality control samples were used to assess the extraction efficiency of the method. For CDD extraction, matrix matched quality control samples included six 1-gram pooled CDD sample produced by combining equal masses of each of the ten distinct CDD components. While for leachate extraction, matrix matched quality control samples included six 50 ml samples made from equal parts of leachate collected from the five L/S= 10 fractions. All samples were extracted the same as their respective sample type, with 40 μL of mass labeled PFAS internal standards (IS) added at different stages. Three of the samples had the IS added before extraction (1-3) while three other samples had the IS added after extraction but before evaporation (4-6).

Supplemental Tables

Table S-1. Lists of native PFAS and corresponding IS for quantification.

	Abbreviation	CAS number	Name	Chemical formula	IS
1	PFBA	375-22-4	perfluorobutanoic acid	$C_4HF_7O_2$	M4PFBA
2	PFPeA	2706-90-3	perfluoropentanoic acid	$C_5HF_9O_2$	M5PFPeA
3	PFHxA	307-24-4	perfluorohexanoic acid	$C_6HF_{11}O_2$	M5PFHxA
4	PFHpA	375-85-9	perfluoroheptanoic acid	$C_7HF_{13}O_2$	M4PFHpA
5	PFOA	335-67-1	perfluorooctanoic acid	$C_8HF_{15}O_2$	M8PFOA
6	PFNA	375-95-1	perfluorononanoic acid	$C_9HF_{17}O_2$	M9PFNA
7	PFDA	335-76-2	Perfluorodecanoic acid	$C_{10}HF_{19}O_2$	M6PFDA
8	PFUdA	2058-94-8	perfluoroundecanoic acid	$C_{11}HF_{21}O_2$	M7PFUdA
9	PFDoA	307-55-1	perfluorododecanoic acid	$C_{12}HF_{23}O_2$	MPFDoA
10	PFTrDA	72629-94-8	perfluorotridecanoic acid	$C_{13}HF_{25}O_2$	M2PFTeDA
11	PFTeDA	376-06-7	perfluorotetradecanoic acid	$C_{14}HF_{27}O_2$	M2PFTeDA
12	PFODA	5339061	perfluorooctadecanoic acid	$C_{18}HF_{35}O_2$	M2PFTeDA
13	PFHxDA	67905-19-5	perfluorohexadecanoic acid	$C_{16}HF_{31}O_2$	M2PFTeDA
14	$PFPrS_{lin,}$	N/A	Sodium perfluoropropane sulfonate	$C_3F_7O_3SNa$	M3PFBS
15	PFBS	29420-49-3	Potassium perfluorobutane sulfonate	$C_4F_9KO_3S$	M3PFBS
16	$PFPeS_{lin,}$	630402-22-1	Sodium perfluoropentane sulfonate	$C_5F_{11}SO_3Na$	M5PFHxA
17	$PFHxS_{lin,}$	82382-12-5	Sodium perfluorohexane sulfonate	$C_6F_{13}NaO_3S$	M3PFHxS
18	$PFHpS_{lin,}$	21934-50-9	Sodium perfluoroheptane sulfonate	$C_7H_{15}FNaO_3S$	M8PFOA
19	$PFOS_{lin,}$	4021-47-0	Sodium perfluorooctane sulfonate	$C_8F_{17}NaO_3S$	M8PFOS
20	$PFNS_{lin,}$	98789-57-2	Sodium perfluorononane sulfonate	$C_9F_{19}NaO_3S$	M2-8:2FTS
21	$PFDS_{lin,}$	2806-15-7	Sodium perfluorodecane sulfonate	$C_{10}F_{21}NaO_3S$	M7PFUdA
22	PFDoS	1260224-54-1	Sodium perfluorododecane sulfonate	$C_{12}F_{25}SO_3Na$	d5-N-EtFOSA-M
23	4:2FTS	27619-93-8	4:2 fluorotelomer sulfonate	$C_6H_4F_9SO_3Na$	M2-4:2FTS
24	6:2FTS	27619-94-9	6:2 fluorotelomer sulfonate	$C_8H_4F_{13}O_3SNa$	M2-6:2FTS
25	8:2FTS	39108-34-4	8:2 fluorotelomer sulfonate	$C_{10}H_4F_{17}NaO_3S$	M2-8:2FTS
26	10:2FTS	108026-35-3	10:2 fluorotelomer sulfonate	$C_{12}H_4F_{21}O_3SNa$	MPFDoA
27	11CI-PF3OUdS	83329-89-9	11-chloroeicosafluoro-3-oxaundecane-1-sulfonate	$C_{10}HClF_{20}O_4SK$	d3-N-MeFOSA-M

Table S-1. Continued.

	Abbreviation	CAS number	Name	Chemical formula	IS
28	9Cl-PF3ONS	73606-19-6	9-chlorohexadecafluoro-3-oxanonane-1-sulfonate	$C_8ClF_{16}KO_4S$	MFOEA
29	NaDONA	958445-44-8	dodecafluoro-3H-4,8-dioxanonanoate	$C_7HF_{12}O_4Na$	M4PFHpA
30	HFPO-DA	13252-13-6	hexafluoropropylene oxide dimer acid (Gen-X)	$C_6HF_{11}O_3$	M3HFPO-DA
31	FBSA-I	30334-69-1	perfluorobutane sulfonamide	$C_4H_2F_9NO_2S$	M2-4:2FTS
32	FHxSA-I	41997-13-1	perfluorohexane sulfonamide	$C_6H_2F_{13}NO_2S$	M2-6:2FTS
33	FOSA-I	754-91-6	perfluoro-1-octanesulfonamide	$C_8H_2F_{17}NO_2S$	M8FOSA
34	N-MeFOSA-M	31506-32-8	N-methylperfluorooctane sulfonamide	$C_9H_4F_{17}NO_2S$	d3-N-MeFOSA-M
35	N-EtFOSA-M	4151-50-2	N-ethylperfluorooctane sulfonamide	$C_{10}H_6F_{17}NO_2S$	d5-N-EtFOSA-M
36	N-AP-FHxSA	50598-28-2	N-(3-dimethylaminopropan-1-yl) perfluoro-1-hexanesulfonamide	$C_{11}H_{13}F_{13}N_2O2S$	MFHEA
37	FOSAA	2806-24-8	2-perfluorooctanesulfonamido acetic acid	$C_{10}H_4F_{17}NO_4S$	M8FOSA
38	N-EtFOSAA	2991-50-6	N-ethylperfluoro-1-octanesulfonamidoacetic acid	$C_{12}H_8F_{17}NO_4S$	d5-N-EtFOSAA
39	N-MeFOSAA	2355-31-9	N-methylperfluoro-1-octanesulfonamidoacetic acid	$C_{11}H_6F_{17}NO_4S$	d3-N-MeFOSAA
40	FHEA	53826-12-3	2-Perfluorohexyl ethanoic acid (6:2)	$C_8H_3F_{13}O_2$	MFHEA
41	FOEA	27854-31-5	2-perfluorooctyl ethanoic acid (8:2)	$C_{10}H_3F_{17}O_2$	MFOEA
42	FDEA	53826-13-4	2-perfluorodecyl ethanoic acid (10:2)	$C_{12}H_3F_{21}O_2$	MFDEA
43	FOUEA	70887-84-2	2H-perfluoro-2-decanoic acid (8:2)	$C_{10}H_2F_{16}O_2$	M9PFNA
44	FDUEA	70887-94-4	2H--perfluoro-2-dcanoic acid (10:2)	$C_{12}H_2F_{20}O_2$	MFDEA
45	6:2diPAP	N/A	sodium bis(1H, 1H, 2H, 2H-perfluorooctyl)phosphate	$C_{16}H_8F_{26}O_4PNa$	M2PFTeDA
46	8:2diPAP	N/A	(1H,1H,2H,2H-perfluorooctyl-1H,1H,2H,2H perfluorodecyl) phosphate	$C_{20}H_8F_{34}NaO_4P$	M2PFTeDA
47	6:2/8:2diPAP	N/A	(1H,1H,2H,2H-perfluorooctyl-1H,1H,2H,2H perfluorodecyl) phosphate	$C_{18}H_8F_{30}NaO_4P$	M2PFTeDA
48	diSAmPAP	N/A	sodium bis-(2-N-ethylperfluorooctane-1-sulfonamido) ethyl	$C_{24}H_{18}F_{34}N_2NaO_8PS_2$	M2PFTeDA
49	8Cl-PFOS	N/A	8-chlorohexadecafluoro-3-oxaoctane-1-sulfonate	$C_8ClF_{16}NaO_3S$	M8PFOS
50	PFECHS	67584-42-3	n-decafluoro-4 ethylcyclohexanesulfonate	C_8F15KO_3S	M2-6:2FTS

Table S-1. Continued.

	Abbreviation	CAS number	Name	Chemical formula	IS
51	N-TAmP-FHxSA,	38850-51-0	N-[3-(perfluoro-1-hexanesulfonamido) propan-1-yl]-N,N,N,trimethylammonium	$C_{12}H_{15}F_{13}N_2O_2S$	M4PFHpA
52	7:2sFTOH	24015-83-6	1-Perfluoroheptyl ethanol (7:2 secondary)	$C_9H_5F_{15}O$	MFOEA
53	5:2sFTOH	914637-05-1	1-Perfluoropentyl ethanol (5:2 secondary)	$C_7H_5F_{11}O$	MFHEA
54	N-CMAmP-6:2FOSA	34455-29-3	N-(carboxymethyl)-N,N-dimethyl-N-[3-(1H,1H,2H,2H-perfluoro-1-octanesulfonamido)propan-1-yl]ammonium (6:2FTAB)	$C_{15}H_{19}F_{13}N_2O_4S$	MFHEA
55	FPrPA (3:3 FTCA)	356-02-5	3-Perfluoropropyl propanoic acid (3:3)	$C_6H_5F_7O_2$	M5PFPeA
56	FPePA (5:3 FTCA)	914637-49-3	3-Perfluoropentyl propanoic acid (5:3)	$C_8H_5F_{11}O_2$	M4PFHpA
57	FHpPA (7:3 FTCA	812-70-4	3-Perfluoroheptyl propanoic acid (7:3)	$C_{10}H_5F_{15}O_2$	M9PFNA
58	PFHxPA	40143-76-8	Perfluorohexylphosphonic acid	$C_6H_2F_{13}O_3P$	M4PFHpA
59	FDSA-I	N/A	Perfluoro-1-decanesulfonamide	$C_{10}H_2F_{21}NO_2S$	MPFDoA
60	N-MeFBSA-M,	68298-12-4	N-methylperfluoro-1-butanesulfonamide	$C_5H_4F_9NO_2S$	M3PFHxS
61	PF4OPeA	377-73-1	Perfluoro-4-oxapentanoic acid (PFMPA)	$C_4HF_7O_3$	M4PFBA
62	3,6-OPFHpA	151772-58-6	Perfluoro-3,6-dioxaheptanoic acid (NFDHA)	$C_5HF_9O_4$	M5PFHxA
63	PFEESA	117205-07-9	Potassium perfluoro(2-ethoxyethane) sulfonate	$C_4F_9KO_4S$	M2-4:2FTS
64	P4MOA ($PFNA_{br}$)	N/A	Perfluoro-4-methyloctanoic acid	$C_9F_{17}HO_2$	M9PFNA
65	NaP3MHpS ($PFOS_{br}$)	N/A	Sodium perfluoro-3-methylheptanesulfonate	$C_8F_{17}SO_3Na$	M8PFOS
66	FHUEA	70887-88-6	2H-Perfluoro-2-octenoic acid (6:2)	$C_8F_{12}O_2H_2$	M4PFHpA
67	6:6PFPi	70609-44-8	Sodium bis(perfluorohexyl) phosphinate	$C_{12}F_{26}PO_2H$	M2PFTeDA
68	6:8PFPi	N/A	Sodium perfluorohexyl perfluorooctylphosphinate	$C_{14}F_{30}PO_2H$	M2PFTeDA
69	Oak 36	2262-49-9	N-n-Propyl-N-(2,3-dihydroxypropyl) perfluorooctyl-sulfonamide	$C_{14}H_{14}F_{17}NO_4S$	d5-N-EtFOSA-M
70	Oak 37	137780-69-9	Perfluoro-3,6-dioxadecanoic acid	$C_8HF_{15}O_4$	M8PFOS
71	Oak 6	1546-95-8	7H-Dodecafluoroheptanoic acid	$C_7H_2F_{12}O_2$	M5PFHxA
72	Oak 8	307-78-8	Hexadecafluorosebacic acid	$C_{10}H_2F_{16}O_4$	M5PFPeA
73	Oak 9 (6:3FTCA),	27854-30-4	2H,2H,3H,3H-Perfluorononanoic acid	$C_9H_5F_{13}O_2$	M8PFOA
74	Oak 10	76-21-1	9H-Hexadecafluorononanoic acid	$C_9H_2F_{16}O_2$	M4PFHpA

Table S-1. Continued.

	Abbreviation	CAS number	Name	Chemical formula	IS
75	Syn2 (EtFHxSE),	34455-03-3	N-Ethyl-N-(2-hydroxyethyl) perfluorohexanesulfonamide	$C_{10}H_{10}F_{13}NO_3S$	M6PFDA
76	Syn28	381-97-5	3,3,3-Trifluoro-2-methylpropionic acid	$C_4H_5F_3O_2$	M4PFBA
77	Syn5(EtFHxSA),	87988-56-5	N-Ethyl perfluorohexylsulfonamide	$C_8H_6F_{13}NO_2S$	M6PFDA
78	Syn32	749836-20-2	7H-Perfluoro-4-methyl-3,6-dioxaoctanesulfonic acid	$C_7H_2F_{14}O_5S$	M4PFHpA
79	Syn34	34642-43-8	Perfluorobutanesulfinic acid	$C_4HF_9O_2S$	M2-4:2FTS
80	Syn35	172155-07-6	Perfluoro-3,7-dimethyloctanoic acid	$C_{10}HF_{19}O_2$	MFOEA
81	Syn12	307-77-7	Perfluorosebacamide	$C_{10}H_4F_{16}N_2O_2$	M5PFHxA
82	Syn38	96513-97-2	Ammonium perfluoro(2-methyl-3-oxaoctanoate)	$C_8H_4F_{15}NO_3$	M8PFOA
83	Syn43	336-08-3	Octafluoroadipic acid	$C_6H_2F_8O_4$	M4PFBA
84	Syn45	678-45-5	Dodecafluorosuberic acid	$C_8H_2F_{12}O_4$	M4PFBA
85	Syn46	103229-89-6	(E)-Perfluoro (4-methylpent-2-noic acid)	$C_6HF_9O_2$	M5PFHxA
86	Syn53	55621-18-6	Perfluoro-3,6,9-trioxaundecane-1,11-dioic acid	$C_8H_2F_{12}O_7$	M5PFPeA
87	Syn58 (8:3FTCA),	34598-33-9	H,2H,3H,3H-Perfluoroundecanoic acid	$C_{11}H_5F_{17}O_2$	M6PFDA
88	Syn59 (HFPO-TeA)	65294-16-8	Perfluoro(2,5,8-trimethyl-3,6,9-trioxadodecanoic) acid	$C_{12}HF_{23}O_5$	MPFDoA
89	Syn62(HFPO-TA)	69105-00-6	2-(Trifluoromethoxy)acetic acid	$C_3H_3F_3O_3$	M4PFBA
90	Syn 68	13252-14-7	Perfluoro (2,5-dimethyl-3,6-dioxanonanoic acid)	$C_9HF_{17}O_4$	MFOEA
91	Syn 71	330562-41-9	Perfluoro-3,6,9-trioxatridecanoic acid	$C_{10}HF_{19}O_5$	d5-N-EtFOSAA
92	Syn 72	70755-50-9	Potassium perfluoro(4-methyl-3,6-dioxaoctane) sulfonate	$C_7F_{15}KO_5S$	M8PFOA

Table S-2. LC-MS/MS operation conditions

Mass Spectrometry Analysis – Thermo Quantis	
Ion Source Parameters	Electrospray – Negative Mode
	Ion Spray: -3000 V
	Sheath Gas: 60 Arb
	Auxiliary Gas: 5 Arb
	Ion Transfer Tube Temperature: 325 °C
	Vaporizer Temperature: 350 °C
Chromatography Conditions – Thermo Scientific Vanquish UHPLC	
LC Conditions	Column: Gemini Phenomenex 100 x 2 mm 3µm
	Gradient Elution using Water and Methanol both containing 5 mM of ammonium acetate
	Oven Temperature 40 °C
	Flow Rate: 0.5 mL min^{-1}
	Injection Volume: 10 µL

Table S-3. Compound-specific method LOD and LOQ

PFAS	MLOD (ng g^{-1})	MLOQ (ng g^{-1})
PFBA	0.006	0.019
PFPeA	0.206	0.687
PFHxA	0.004	0.014
PFHpA	0.041	0.137
PFOA	0.015	0.049
PFNA	0.023	0.076
PFDA	0.012	0.040
PFUdA	0.012	0.042
PFDoA	0.006	0.019
PFTrDA	0.015	0.051
PFTeDA	0.004	0.014
PFODA	0.007	0.025
PFHxDA	0.012	0.041
L-PFPrS	0.046	0.154
L-PFBS	0.009	0.028
L-PFPeS	0.388	1.293
∑PFHxS	0.126	0.419
L-PFHpS	0.131	0.436
L-PFOS	0.025	0.084
Br-PFOS	0.012	0.041
L-PFNS	0.040	0.132
L-PFDS	0.025	0.083
L-PFDoS	0.117	0.390
4:2FTS	0.012	0.042
6:2FTS	0.008	0.026
8:2FTS	0.016	0.053
10:2FTS	0.034	0.113
11CI-PF3OUdS	0.008	0.026
9Cl-PF3ONS	0.008	0.027
NaDONA	0.005	0.018
HFPO-DA	0.412	1.374
FBSA	0.008	0.027
FHxSA	0.082	0.275
FOSA	0.016	0.055
N-MeFOSA-M	0.363	1.210
N-EtFOSA-M	0.180	0.600
N-AP-FHxSA	0.300	1.001
FOSAA	0.013	0.045

N-EtFOSAA	0.014	0.046
N-MeFOSAA	0.012	0.042
FHEA	0.078	0.260
FOEA	0.039	0.129
FDEA	0.031	0.102
FDUEA	0.009	0.031
FOUEA	0.014	0.045
6:2diPAP	0.004	0.012
8:2diPAP	0.018	0.061
6:2/8:2diPAP	0.035	0.118
diSAmPAP	0.036	0.120
8Cl-PFOS	0.086	0.287
PFECHS	0.039	0.129
N-TAmP-FHxSA	0.111	0.370
N-CMAmP-6:2FOSA	0.164	0.545
7:2sFTOH	0.363	1.211
5:2sFTOH	0.166	0.553
FPrPA	0.123	0.411
FPePA	0.074	0.247
FHpPA	0.029	0.096
PFHxPA	0.123	0.410
FDSA-I	0.065	0.217
MeFBSA-M	0.371	1.237
PF4OPeA	0.181	0.605
3,6-OPFHpA	0.007	0.024
PFEESA	0.026	0.088
P4MOA	0.030	0.102
N-MeFOSE-M	0.071	0.237
N-EtFOSE-M	0.171	0.570
FHUEA	0.129	0.429
6:6PFPi	0.011	0.037
6:8PFPi	0.007	0.025
Oak 36	0.206	0.687
Oak 2	0.196	0.653
Oak 37	0.004	0.013
Oak 6	0.014	0.047
Oak 8	0.033	0.109
Oak 9	0.135	0.448
Oak 10	0.008	0.026
Syn2	0.398	1.325

Syn28	0.071	0.236
Syn5	0.039	0.129
Syn32	0.028	0.094
Syn34	0.015	0.050
Syn35	0.076	0.255
Syn12	0.070	0.233
Syn38	0.133	0.444
Syn41	0.020	0.066
Syn43	0.013	0.042
Syn45	0.008	0.026
Syn46	0.058	0.194
Syn53	0.011	0.037
Syn58	0.077	0.255
Syn59	0.360	1.201
Syn62	0.345	1.150
Syn68	0.117	0.391
Syn71	0.007	0.024
Syn72	0.010	0.034

Table S-4. Extraction efficiency results for detected PFAS in solids and liquids.

Compound	Solids extraction efficiency (%)	Liquid extraction efficiency (%)
PFBA	104	86
PFPeA	97	88
PFHxA	83	109
PFHpA	86	92
PFOA	94	98
PFNA	82	90
PFDA	75	78
PFUnDA	74	70
PFDoDA	74	50
PFTeDA	83	60
PFTrDA	78	59
PFHxDA	69	67
PFODA	66	56
PFBS	85	102
PFHxS	75	85
PFOS	90	85
PFNS	67	91
PFDS	65	75
4:2FTS	62	99
6:2FTS	72	85
8:2FTS	68	94
10:2FTS	85	68
6:6PFPi	66	53
6:8PFPi	76	55
6:2diPAP	95	69
6:2/8:2diPAP	68	53
8:2diPAP	63	104
FOSA	70	78
d3-N-MeFOSA-M	50	61
d5-N-EtFOSA-M	76	74
MeFOSAA	53	82
EtFOSAA	62	74
Oak6	73	100
Syn34	101	85
PFECHS	112	101
Syn35	78	84
diSamPAP	43	48
Average	78	79

Table S-5. Total available PFAS concentrations detected in nine major CDD waste. Metals were not analyzed for total available PFAS concentrations as size reduction was infeasible. Units are in ng/g. Only the compounds detected in all triplicates are reported. Two significant figures are reported.

PFAS	Concrete	Mixed wood	RAP	Cardboard	Carpet padding	Carpet	CDD fines	Gypsum drywall	Asphalt shingles
PFBA	0.094	0.18	<LOQ	<LOQ	1.1	<LOQ	0.26	6.5	<LOQ
PFPeA	<LOQ	<LOQ	<LOQ	<LOQ	<LOQ	<LOQ	2.3	<LOQ	<LOQ
PFHxA	0.18	22	<LOQ	<LOQ	1.7	<LOQ	2.1	29	1.1
PFHpA	<LOQ	0.65	0.20	<LOQ	0.65	<LOQ	0.56	0.54	0.13
PFOA	0.16	<LOQ	<LOQ	0.10	3.2	0.27	1.1	1.4	0.37
∑PFNA	<LOQ	0.70	<LOQ	<LOQ	<LOQ	<LOQ	0.2	0.26	<LOQ
PFDA	0.10	<LOQ	<LOQ	<LOQ	0.68	<LOQ	0.45	0.27	<LOQ
PFUdA	0.032	<LOQ	<LOQ	0.049	0.15	<LOQ	0.10	0.063	<LOQ
PFDoA	0.084	<LOQ	<LOQ	0.028	0.31	<LOQ	0.22	0.14	<LOQ
PFTrDA	<LOQ	<LOQ	<LOQ	<LOQ	<LOQ	<LOQ	0.024	0.047	<LOQ
PFTeDA	<LOQ	<LOQ	<LOQ	<LOQ	<LOQ	<LOQ	0.094	0.11	<LOQ
PFHxDA	<LOQ	<LOQ	<LOQ	<LOQ	<LOQ	<LOQ	0.028	<LOQ	<LOQ
PFBS	0.13	<LOQ	<LOQ	<LOQ	1.4	<LOQ	0.68	<LOQ	<LOQ
PFHxS	<LOQ	<LOQ	<LOQ	<LOQ	4.2	<LOQ	0.93	<LOQ	<LOQ
∑PFOS	0.19	0.033	<LOQ	0.11	7.3	0.48	1.3	1.3	<LOQ

Table S-5. Continued.

PFAS	Concrete	Mixed wood	RAP	Cardboard	Carpet padding	Carpet	CDD fines	Gypsum drywall	Asphalt shingles
PFDS	<LOQ	<LOQ	<LOQ	<LOQ	0.28	<LOQ	0.19	<LOQ	<LOQ
Syn34	<LOQ	<LOQ	<LOQ	<LOQ	4.1	<LOQ	<LOQ	<LOQ	<LOQ
Oak6 (7H-PFHpA)	<LOQ	0.29	<LOQ	<LOQ	0.51	<LOQ	<LOQ	<LOQ	<LOQ
6:2 FTS	1.9	5.0	0.84	15.1	110	21	14	13	15
10:2 FTS	<LOQ	<LOQ	<LOQ	<LOQ	0.81	<LOQ	0.14	0.36	<LOQ
Syn5 (EtFHxSA)	<LOQ	<LOQ	<LOQ	<LOQ	<LOQ	160	<LOQ	<LOQ	<LOQ
MeFOSAA	<LOQ	<LOQ	<LOQ	<LOQ	<LOQ	<LOQ	2.0	<LOQ	<LOQ
EtFOSAA	<LOQ	<LOQ	<LOQ	0.11	12	0.93	1.2	1.2	<LOQ
6:8PFPi	<LOQ	<LOQ	<LOQ	<LOQ	0.15	<LOQ	<LOQ	<LOQ	<LOQ
6:2diPAP	<LOQ	<LOQ	<LOQ	0.22	<LOQ	<LOQ	3.0	0.58	<LOQ
6:2/8:2diPAP	0.13	1.1	<LOQ	2.4	13	2.1	14	42	0.59
8:2diPAP	<LOQ	<LOQ	<LOQ	0.76	1.3	0.55	3.9	22	0.12
Syn35	<LOQ	<LOQ	<LOQ	<LOQ	0.25	0.062	0.14	0.10	<LOQ
diSAmPAP	<LOQ	0.12	<LOQ	2.4	1.9	<LOQ	1.2	0.43	0.70
$\sum_{92}$PFAS	3.0	30	1.0	21	170	190	50	120	18

Table S-6. Leachable PFAS concentrations detected in 10 major CDD waste using nanopure water leaching. Units are in ng/g. Only the compounds detected in all replicates are reported. Two significant figures are reported.

PFAS	Concrete	Mixed wood	RAP	Cardboard	Carpet padding	Carpet	CDD fines	Gypsum drywall	Asphalt shingles	Metals
PFBA	0.13	0.15	<LOQ	<LOQ	0.35	0.22	0.28	0.85	<LOQ	0.13
PFPeA	0.077	<LOQ	<LOQ	<LOQ	<LOQ	<LOQ	2.1	<LOQ	<LOQ	
PFHxA	0.14	5.7	<LOQ	0.34	0.13	0.20	1.5	9.1	<LOQ	<LOQ
PFHpA	<LOQ	<LOQ	<LOQ	<LOQ	<LOQ	0.055	1.6	0.19	<LOQ	<LOQ
PFOA	0.13	0.039	<LOQ	0.060	0.020	0.13	0.78	0.88	0.019	0.11
∑PFNA	0.025	0.088	<LOQ	<LOQ	<LOQ	0.012	0.10	0.045	<LOQ	<LOQ
PFDA	0.060	<LOQ	<LOQ	<LOQ	<LOQ	<LOQ	0.057	0.16	<LOQ	<LOQ
PFUdA	<LOQ	<LOQ	<LOQ	<LOQ	<LOQ	<LOQ	<LOQ	0.018	<LOQ	<LOQ
PFBS	0.10	0.017	<LOQ	0.038	0.03	0.23	0.36	<LOQ	<LOQ	<LOQ
PFHxS	0.015	<LOQ	<LOQ	<LOQ	<LOQ	0.099	0.54	<LOQ	<LOQ	<LOQ
∑PFOS	0.088	0.025	<LOQ	0.016	<LOQ	<LOQ	0.21	0.73	0.011	0.056
Syn34	0.039	<LOQ	<LOQ	<LOQ	0.22	<LOQ	<LOQ	<LOQ	<LOQ	<LOQ
Oak6 (7H-PFHpA)	<LOQ	<LOQ	<LOQ	<LOQ	<LOQ	0.030	<LOQ	0.085	<LOQ	<LOQ
6:2 FTS	0.062	0.35	0.11	0.32	0.36	0.33	0.19	0.48	0.14	<LOQ

Table S-6. Continued.

PFAS	Concrete	Mixed wood	RAP	Cardboard	Carpet padding	Carpet	CDD fines	Gypsum drywall	Asphalt shingles	Metals
Syn5 (EtFHxSA)	<LOQ	<LOQ	<LOQ	<LOQ	<LOQ	0.48	<LOQ	<LOQ	<LOQ	<LOQ
MeFOSAA	<LOQ	<LOQ	<LOQ	<LOQ	<LOQ	<LOQ	0.25	<LOQ	<LOQ	<LOQ
Syn35	0.018	<LOQ	<LOQ	<LOQ	<LOQ	0.0094	0.022	0.062	<LOQ	<LOQ
$\sum_{92}$PFAS	0.88	6.37	0.11	0.77	1.1	1.8	8.0	13	0.17	0.30

Table S-7. Leachable PFAS concentrations detected in 10 major CDD waste using TCLP. Units are in ng/g. Only the compounds detected in all replicates are reported. Two significant figures are reported.

PFAS	Concrete	Mixed wood	RAP	Cardboard	Carpet padding	Carpet	CDD fines	Gypsum drywall	Asphalt shingles	Metals
PFBA	0.16	0.98	<LOQ	<LOQ	0.21	0.22	0.37	1.8	<LOQ	<LOQ
PFPeA	0.15	<LOQ	<LOQ	<LOQ	<LOQ	<LOQ	1.4	<LOQ	<LOQ	<LOQ
PFHxA	0.090	2.8	<LOQ	<LOQ	0.061	0.14	0.95	3.1	0.16	<LOQ
PFHpA	<LOQ	<LOQ	<LOQ	<LOQ	<LOQ	<LOQ	0.21	0.19	<LOQ	<LOQ
PFOA	0.14	0.028	<LOQ	0.044	0.0073	0.10	0.42	0.71	0.015	<LOQ
∑PFNA	0.040	<LOQ	<LOQ	<LOQ	<LOQ	<LOQ	0.072	0.030	<LOQ	<LOQ
PFDA	0.058	<LOQ	<LOQ	<LOQ	<LOQ	<LOQ	0.041	0.12	<LOQ	<LOQ
PFUdA	<LOQ	<LOQ	<LOQ	<LOQ	<LOQ	<LOQ	<LOQ	<LOQ	<LOQ	<LOQ
PFBS	0.070	<LOQ	<LOQ	<LOQ	<LOQ	<LOQ	0.26	<LOQ	<LOQ	<LOQ
PFHxS	<LOQ	<LOQ	<LOQ	<LOQ	<LOQ	<LOQ	0.23	<LOQ	<LOQ	<LOQ
∑PFOS	0.10	<LOQ	<LOQ	<LOQ	<LOQ	0.10	0.15	0.44	<LOQ	<LOQ
Syn34	0.066	<LOQ	<LOQ	<LOQ	0.36	<LOQ	<LOQ	<LOQ	<LOQ	<LOQ
Oak6 (7H-PFHpA)	<LOQ	<LOQ	<LOQ	<LOQ	<LOQ	0.030	<LOQ	0.085	<LOQ	<LOQ
6:2 FTS	0.62	0.32	0.26	0.70	0.36	0.41	<LOQ	1.3	0.38	<LOQ

Table S-7. Continued.

PFAS	Concrete	Mixed wood	RAP	Cardboard	Carpet padding	Carpet	CDD fines	Gypsum drywall	Asphalt shingles	Metals
Syn5 (EtFHxSA)	<LOQ	<LOQ	<LOQ	<LOQ	<LOQ	0.51	<LOQ	<LOQ	<LOQ	<LOQ
MeFOSAA	<LOQ	<LOQ	<LOQ	<LOQ	<LOQ	<LOQ	<LOQ	<LOQ	<LOQ	<LOQ
EtFOSAA	<LOQ	<LOQ	<LOQ	<LOQ	<LOQ	0.20	<LOQ	0.16	<LOQ	<LOQ
Syn35	0.024	<LOQ	<LOQ	<LOQ	<LOQ	<LOQ	0.021	0.051	<LOQ	<LOQ
$\sum_{92}$PFAS	1.5	4.1	0.26	0.74	1.0	1.7	4.1	8.0	0.56	<LOQ

Table S-8. Data and corresponding sources utilized for national CDD extrapolation.

Item	Extrapolation Assumption			Source
CDD generation	1.84 Mg capita^{-1} year^{-1}			Townsend and Anshassi (2023)
US population (2023)	335,000,000			US Census Bureau (2020)
States without CDD landfill liner requirements	AK, AZ, CT, FL, GA, ID, IL, KS, ME, MN, NE, NV, NM, NC, ND, SC, SD, TN, UT, VT, WV, WY			Clark et al. (2006)
US CDD	% Composition	% Landfilled	% Recycled/next use	US EPA (2017)
Concrete	67.5	17.6	82.4	
Asphalt	17.8	4.6	95.4	
Wood products	6.8	72.5	27.5	
Drywall and plaster	2.5	86.3	13.7	
Shingles	2.5	86.1	13.9	
Brick and tile	2.0	87.8	12.2	
Steel/Metal	0.8	23.4	76.6	

National PFAS load from CDD

$$= \left(\sum_{n = \text{Alabama}}^{\text{Wyoming}} \frac{\text{Mg CDD generated}}{\text{capita}}^{a} \text{ x capita}_n{}^{b} \right) \text{x} \left(\sum_{n=\text{Concrete}}^{\text{Steel or metal}} \%\ \text{composition}_n^c \text{ x total extractable PFAS}_n^d \right)$$

$$\text{National PFAS disposal fate from CDD} = \left(\sum_{n=\text{Concrete}}^{\text{Steel or metal}} \text{National PFAS load from CDD}_n \text{ x } \%\ \text{landfilled or recycled}_n^c \right)$$

PFAS disposed to unlined landfill from CDD

$$= \frac{\text{Mg CDD generated in states without CDD landfill liner requirements}}{\text{Mg CDD generated in states with any CDD landfill liner requirements}}^{e} \text{ x National PFAS disposal to landfill from CDD}$$

a. Townsend and Anshassi (2023)
b. US Census Bureau
c. US EPA (2017)
d. This study
e. Clark et al. (2006)

References:

(1) Townsend, T.G., Anshassi, M., 2023. Construction and Demolition Debris, Waste Management Principles and Practice. Springer International Publishing, Cham. https://doi.org/10.1007/978-3-031-25013-2

(2) US Census Bureau, 2020. State Population Totals and Components of Change: 2020-2023.

(3) US EPA, O., 2017. Construction and Demolition Debris: Material-Specific Data. URL https://www.epa.gov/facts-and-figures-about-materials-waste-and-recycling/construction-and-demolition-debris-material (accessed 12.12.23).

(4) Clark, C., Jambeck, J., Townsend, T., 2006. A Review of Construction and Demolition Debris Regulations in the United States. Crit. Rev. Environ. Sci. Technol. 36, 141–186. https://doi.org/10.1080/10643380500531197